Title

Optimizing the Hemoglobin-Based Oxygen Carrier Molecular Size to Balance Vascular Function and Hemodynamic Responses after Transfusion

Journal

ACS Applied Bio Materials

ISSN

2576-6422

Authors

Munoz, Carlos

Lucas, Daniela

Martinez, Jacinda

et al.

Publication Date

2026-07-24

DOI

10.1021/acsabm.6c00900

ACS APPLIED BIO MATERIALS

www.acsabm.org Article

Optimizing the Hemoglobin-Based Oxygen Carrier Molecular Size to Balance Vascular Function and Hemodynamic Responses after Transfusion

Carlos Munoz, Daniela Lucas, Jacinda Martinez, Nathaniel Ung, Mohd Asim Khan, Tanmay Salvi, Griffin J. Beyer, Andre F. Palmer, and Pedro Cabrales*

Cite This: https://doi.org/10.1021/acsabm.6c00900 Read Online

ACCESS | Metrics & More | Article Recommendations | Supporting Information

ABSTRACT: Hemorrhagic shock remains a leading cause of mortality due to impaired oxygen delivery following severe blood loss. Hemoglobin-based oxygen carriers (HBOCs) are promising alternatives to red blood cell transfusion; however, their molecular size critically governs nitric oxide (NO) scavenging, vascular reactivity, and overall safety. Here, we systematically evaluated acellular human hemoglobin (hHb) and four polymerized hemoglobin formulations with progressively increasing molecular weights (PolyhHb-10, ∼1080 kDa; PolyhHb-12, ∼1200 kDa; PolyhHb-15, ∼1490 kDa; and PolyhHb-16, ∼1570 kDa) to define size-dependent determinants of vascular function. Ex vivo, isolated mesenteric arterioles from New Zealand white rabbits were perfused with HBOC−whole blood mixtures (1:0, 1:1, and 1:3) across physiologically relevant flow rates to quantify shear-mediated vasodilation and endothelial function. The acetylcholine challenge was used to probe NO bioavailability. In vivo validation was performed in Golden Syrian hamsters using a dorsal window chamber model to assess microvascular hemodynamics, including the vessel diameter, blood flow, and functional capillary density. PolyhHb-12 consistently preserved endothelial-dependent vasodilation and exhibited minimal NO scavenging across conditions. In contrast, larger polymers (PolyhHb-15 and PolyhHb-16) showed paradoxically increased NO scavenging despite improved capillary perfusion, indicating a trade-off between microcirculatory flow enhancement and endothelial signaling. In vivo, increasing the molecular size yielded diminishing returns in overall hemodynamic stability. Together, these findings identify an intermediate molecular size as optimal for balancing rheological properties, NO bioavailability, and vascular function. PolyhHb-12 emerges as a lead candidate, supporting the design of next-generation HBOCs with improved safety and efficacy for hemorrhagic shock resuscitation.

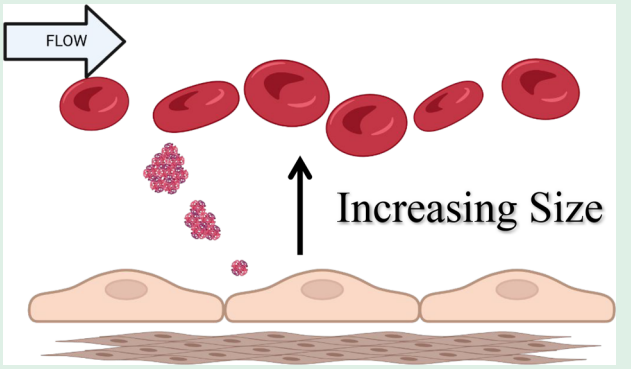

KEYWORDS: *hemoglobin-based oxygen carriers, polymerization characteristics, microcirculation, influences on blood flow profiles, fluid dynamics, nitric oxide scavenging*

INTRODUCTION

Hemorrhage, or uncontrolled bleeding, is a critical medical challenge in both military and civilian settings. Severe blood loss leads to hypovolemia, reduced blood flow, and diminished oxygen (O_2) delivery to tissues, which subsequently causes cellular apoptosis and necrosis in tissues and vital organs, ultimately leading to multiorgan failure and eventually death.[1−3] In hospital conditions, traditional whole blood or red blood cell (RBC) transfusions sourced from allogenic donated blood are the current gold standard to treat hemorrhage.[3−5] However, in prehospital emergency settings, battle field, and during natural disasters, severely injured individuals often bleed out before reaching medical facilities, with a significant number of trauma-related deaths occurring before patients receive medical attention or arrive at a facility equipped to provide blood transfusions. Deep et al. found that every 1 min delay in time to early resuscitative intervention was associated with a 2% increase in the odds of 30-day mortality.[2]

Many institutions are attempting to incorporate whole blood resuscitation in prehospital environments,[3,4] but the integrity of whole blood products is difficult to maintain even in hospital conditions. Whole blood requires refrigeration and has a prohibitively short shelf life of 21–35 days, depending on the anticoagulant

Received: May 6, 2026
Revised: July 15, 2026
Accepted: July 20, 2026

used.[5,6] Transport failures (e.g., inappropriate storage, delayed transport, or damage) or blood mishandling at the site of transfusion (e.g., failed intravenous access and inadequate consent) are the primary drivers of blood product waste or delayed transfusion.[7] Furthermore, whole blood transfusion requires blood type matching, which is another limitation to whole blood's convenience in hemorrhagic trauma scenarios. It is estimated that between 60,000 and 300,000 patients in prehospital care situations every year in the United States would benefit from a resuscitative fluid capable of transporting and delivering oxygen (O_2).[4]

Alternative O_2-carrying solutions are mostly based on hemoglobin (Hb) as the precursor and are known as Hb-based O_2 carriers (HBOCs).[8] HBOCs have been developed to restore tissue perfusion and oxygenation when blood is not an option. An ideal HBOC should provide universal compatibility, prolonged storage stability, and a favorable safety profile while effectively transporting oxygen. However, despite substantial advances in HBOC development, vascular complications associated with NO scavenging and altered microvascular hemodynamics remain major barriers to clinical translation. Accordingly, the present study focuses specifically on the influence of PolyhHb molecular size on vascular compatibility and hemodynamic responses.

To overcome these challenges, the primary mitigation strategy has involved creating polymers of Hb, whose increased molecular weight and size limit Hb's native tendency toward dissociation into dimers and monomers and prevent extravasation of the molecule into the interstitial space, thereby avoiding the worst adverse effects associated with utilizing HBOCs. Hb polymerization confers additional advantages such as reducing heme release and increasing its circulatory half-life.[9−13]

Despite decades of research on hemoglobin-based oxygen carriers (HBOCs), the optimal polymer molecular size that balances vascular safety with effective oxygen delivery remains poorly defined. While increasing polymer size has the potential to reduce hemoglobin extravasation and nitric oxide (NO) scavenging, it may also alter rheological properties and microvascular blood flow. In this study, we evaluated four polymerized human hemoglobin (PolyhHb) formulations with progressively increasing molecular weight (PolyhHb-10, PolyhHb-12, PolyhHb-15, and PolyhHb-16) to determine how polymer size influences vascular function and systemic hemodynamic responses. We hypothesized that increasing the PolyhHb molecular weight would reduce NO scavenging and attenuate vasoconstriction, thereby improving vascular compatibility, microvascular blood perfusion, and overall hemodynamic stability. To test this hypothesis, we used an ex vivo isolated small-arteriole perfusion model to quantify flow-mediated vasoreactivity under varying shear conditions and HBOC-to-whole blood ratios, followed by in vivo validation in Golden Syrian hamsters fitted with a dorsal window chamber to assess microvascular diameter, blood flow, and functional capillary density. Together, these complementary studies were designed to identify the optimal PolyhHb molecular size for preserving vascular function and guiding the rational design of next-generation HBOCs.

METHODS

Polymerized Human Hemoglobin (PolyhHb) Synthesis and Characterization

Polymerized human Hb (PolyhHb) formulations were produced from purified stroma-free human Hb (hHb) using a controlled polymerization and tangential flow filtration (TFF) purification process as previously described in the literature.[14]

PolyhHb molecular weight distribution was estimated by size-exclusion chromatography (Figure 1), and key physicochemical properties, including the molecular diameter, metHb fraction, oxygen affinity (P_{50}, partial pressure of oxygen where half of the Hb is saturated with oxygen), and cooperativity coefficient (n), were characterized (Table 1). All formulations were adjusted to matched Hb concentrations prior to experimental testing. Half-life values were determined in C57BL/6 mice following a single intravenous administration of hHb or PolyhHb formulations (10 g/dL). The administered volume corresponded to 10% of the estimated blood volume (7% of body weight). Plasma hemoglobin concentrations were quantified from serial tail vein blood samples collected over 8 h, and half-lives were calculated by fitting the plasma concentration–time profiles. Methemoglobin (metHb) concentration was determined spectrophotometrically using a NanoDrop spectrophotometer by measuring absorbance at 630 nm. During the autooxidation measurements, samples remained at rest in the cuvette without stirring.

Isolated Blood Vessel Preparation

All isolated blood vessel experiments were conducted using New Zealand white rabbits in accordance with protocols approved by the Institutional Animal Care and Use Committee (IACUC). Briefly, rabbits were anesthetized using isoflurane (5% induction, 2% maintenance, Drägerwerk AG, Lübeck, Germany) and euthanized with an overdose of sodium pentobarbital (150 mg/kg IV). Following euthanasia, mesenteric arteries (300–400 μm diameter) were rapidly dissected, excised, and transferred to a refrigerated (4 °C) physiological salt solution (PSS: NaCl 119 mM, KCl 4.7 mM, $CaCl_2$ 2.5 mM, $MgSO_4$ 1.17 mM, $NaHCO_3$ 25 mM, KH_2PO_4 1.18 mM, EDTA 0.026 mM, and glucose 5.5 mM, pH 7.4). Blood vessels were cannulated onto glass micropipettes within a blood vessel chamber (Living Systems Instrumentation, Burlington, VT) filled with physiological salt solution (PSS) maintained at physiological temperature (37 °C).

Isolated Blood Vessel Perfusion System

The blood vessel perfusion system (Living Systems Instrumentation, Burlington, VT) consisted of a temperature-controlled superfusion bath, a servo-controlled pressure monitor, video microscopy coupled with a video dimension analyzer (V94, Living Systems Instrumentation), and continuous data acquisition systems. The isolated blood vessels were

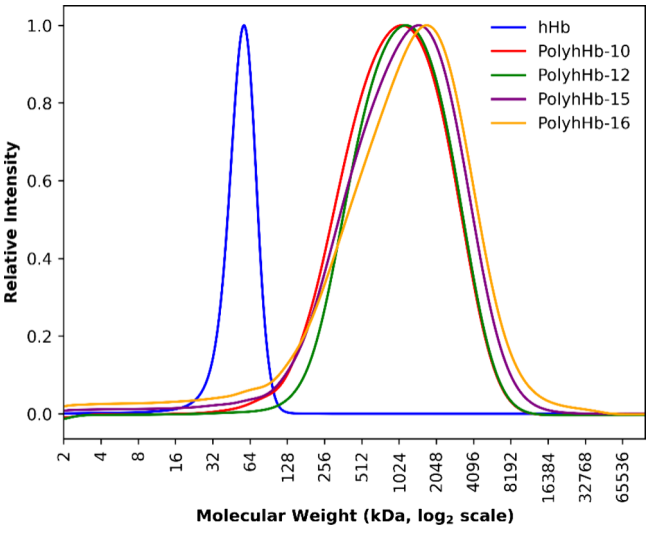

Figure 1. Size distribution of polymerized hemoglobin solutions. The hemoglobin solution utilized for resuscitation was analyzed using size-exclusion chromatography.

https://doi.org/10.1021/acsabm.6c00900
ACS Appl. Bio Mater. XXXX, XXX, XXX−XXX

Table 1. HBOC Characteristics

Product name	hHb	PolyhHb-10	PolyhHb-12	PolyhHb-15	PolyhHb-16
Hemoglobin type	Human	Human	Human	Human	Human
Hb purity (%)	98	98	98	98	98
Non-Hb components	Modified Ringer's lactate: DI water (balance), NaCl, 6.7g/L; NALC, 2.1 g/L;$CaCl_{2.2}(H_2O)$, 0.2 g/L; KCl, 0.3 g/L; NaOH, 0.5 g/L; NaLac, 3.8 mL/L				
Molecular weight (kDa)	64	1078	1200	1490	1569
Half-life (h)	1.008	7.38	5.821	4.394	3.727
Molecular diameter (nm)	6	28	38	55	67
MetHb level(%)	6.3	1.3	3.9	3.0	2.3
P_{50} (mmHg)	15.27	37.95	47.3	44.4	42.2
Cooperativity coefficient	2.37	0.86	0.98	0.71	1.10

pressurized to a mean physiological pressure of 60 mmHg and allowed to equilibrate for 30 min under low-flow conditions (3 μL/s). Blood vessel reactivity was assessed by constriction with extraluminal application of noradrenaline (NA, 1 μmol/L) in potassium (64 mmol/L)-substituted PSS and subsequent dilatation with acetylcholine (ACh, 1 μmol/L). The flow pump had been previously calibrated, and the relationship between proximal pressure and flow rate was found to be linear over the flow rate range.

HBOC Perfusion Experiments

Prior to perfusion experiments, PSS was removed from the circuit. Polymerized HBOCs (PolyhHb-10, PolyhHb-12, PolyhHb-15, and PolyhHb-16) were mixed with fresh whole rabbit blood collected in citrate-phosphate-dextrose (CPD) at volume:volume ratios of 1:0 (HBOC only), 1:1 (HBOC:fresh whole blood), and 1:3 (HBOC:fresh whole blood). Fresh rabbit whole blood was used as a positive control. These volume:volume ratios were chosen to mimic clinically relevant scenarios of partial or full resuscitation from hemorrhagic shock. Rabbit blood was standardized to a hematocrit of 25% using fresh rabbit plasma before mixing with HBOCs to ensure consistency with blood rheological and oxygen-carrying capacity properties. Each HBOC–blood mixture was perfused into the isolated blood vessel at controlled flow rates (3, 5, 8, 10, and 15 μL/s) to simulate physiological flows and shear stresses relevant to arterioles of comparable size and to document the flow-mediated dilation produced by endothelial mechanotransduction. The imposed flow conditions were selected to test whether each PolyhHb formulation altered the normal dilation of resistance vessels in response to endothelial shear stimulation. Hemodynamic shear stresses on the endothelium lead to biophysical, biochemical, and gene regulatory responses on endothelial cells in response to flow-derived shear stresses on the endothelium that mediate autocoid synthesis and release responsible for smooth muscle relaxation. The detailed experimental setup is shown in Figure 2.

Blood Vessel Diameter Measurements

Changes in the blood vessel diameter in response to changes in blood flow rates and HBOC formulations were measured continuously by video microscopy, with the data recorded in real-time using a video dimension analyzer. Percent vasodilation was calculated as a percentage change from the initial blood vessel diameter prior to HBOC perfusion.

NO-Mediated Dilation Experiments

To assess endothelial-dependent NO-mediated dilation, a trace amount of ACh (1 μmol/L final concentration using a syringe infusion pump) was introduced concurrently with HBOC–blood mixtures at a constant low flow rate of 3 μL/s. The arteriolar vessel diameter changes were recorded to evaluate the NO scavenging effects of HBOC formulations and assess endothelial function and NO bioavailability.

In Vivo Evaluation

Male Golden Syrian hamsters (55–65 g; Charles River Laboratories, Boston, MA) were implanted with a dorsal skinfold window chamber and vascular catheters in the jugular vein and carotid artery. All animal procedures were approved by the University of California San Diego Institutional Animal Care and Use Committee (IACUC; Protocol S04052) and conducted in accordance with the NIH Guide for the Care and Use of Laboratory Animals and applicable USDA regulations. The dorsal skinfold window chamber is a well-established model for investigating the microcirculation in conscious animals, and the complete surgical procedure has been described previously.[15,16] Briefly, a dorsal skinfold window chamber was surgically implanted by creating a 2.5 cm skin fold on the dorsal surface. A circular region (1.5 cm diameter) of the skin and underlying tissue was removed from one side of the fold to expose the underlying microvasculature, and the overlying fascia was carefully retracted to optimize optical access for intravital imaging.

To reduce restraint-related stress during conscious imaging, hamsters were habituated to the restraining tube by placing the tube in their home cage for at least three days before experimentation, allowing voluntary exploration. Following window chamber implantation and vascular catheterization, the restraining tube was removed from the cage to avoid interference with recovery. Experiments were performed one day after catheterization to confirm catheter patency. Animals were allowed to recover before imaging, and only preparations exhibiting normal tissue appearance without bleeding, edema, inflammation, or impaired microvascular perfusion were included in the study.

Inclusion Criteria

Animals were suitable for the experiments if (1) systemic variables were within a normal range, namely, heart rate (HR) > 340 beat/min, mean arterial blood pressure (MAP) > 80 mmHg, systemic hematocrit (Hct) > 45%, and arterial oxygen partial pressure (PaO_2) > 50 mmHg; and (2) microscopic examination of the tissue in the chamber observed under a 650× magnification did not reveal signs of edema or bleeding. Hamsters are a fossorial species with a lower arterial PO_2 than other rodents due to their adaptation to a subterranean environment. However, microvascular PO_2 distribution in the chamber window model is the same as in other rodents such as mice.[17]

Hypervolemic Infusion (Top-Load) Protocol

Experimental groups were labeled based on a hypervolemic infusion corresponding to 10% of the animal's estimated blood volume (assuming that the blood volume is 7% of the total body weight), equivalent to 7 mL/kg body weight. Experimental groups included hHb as a negative control, 10% human serum albumin (HSA) as a positive control, and PolyhHb-10, PolyhHb-12, PolyhHb-15, and PolyhHb-16 ($n = 6$ animals per group). All infused solutions were standardized to a total protein concentration of 10 g/dL. HBOCs and hHb were administered over approximately 2 min through the carotid artery. After infusion, animals were allowed to stabilize for 30 min before systemic and microvascular characterization. The experimental timeline is described in Figure S1.

https://doi.org/10.1021/acsabm.6c00900
ACS Appl. Bio Mater. XXXX, XXX, XXX–XXX

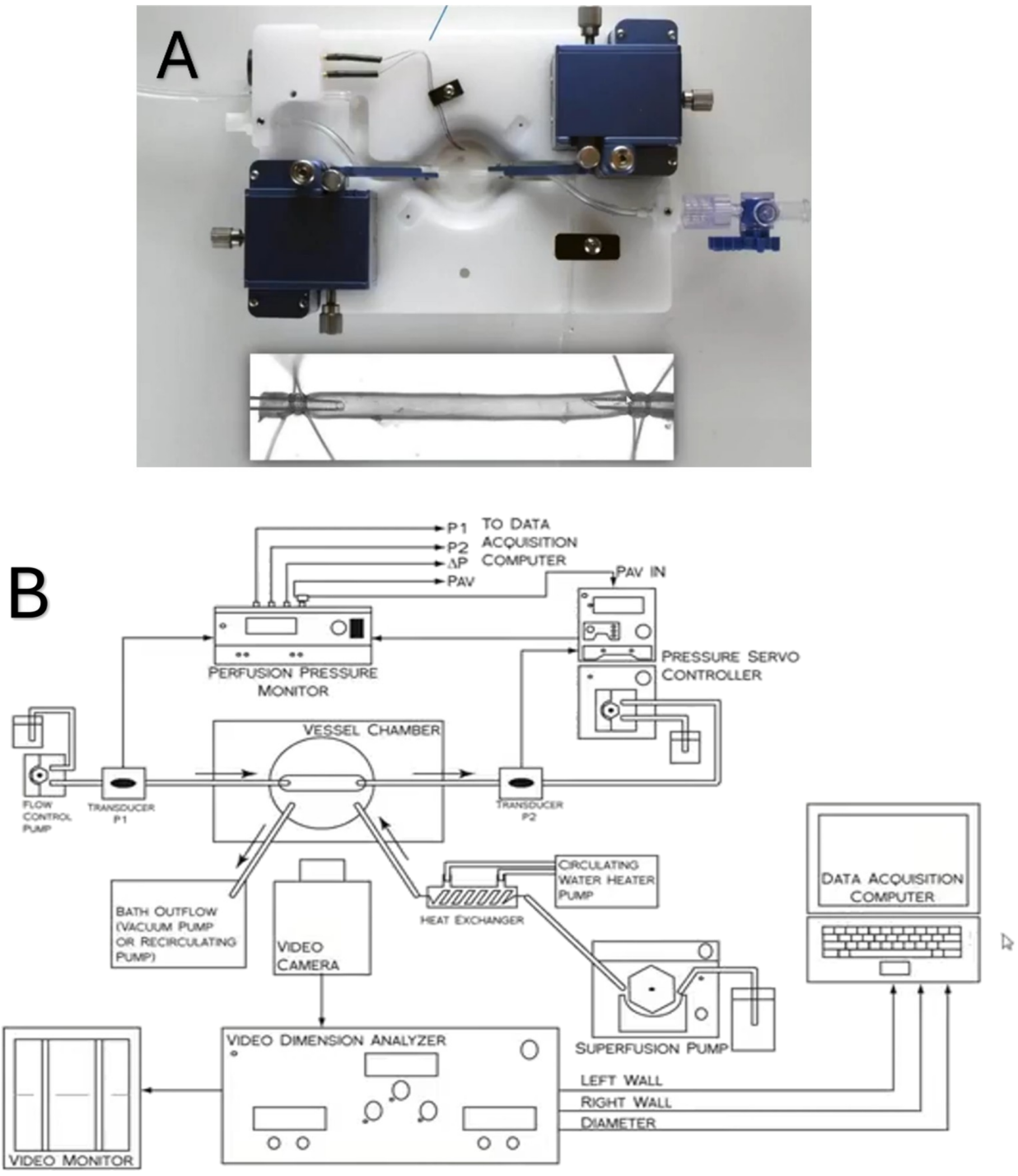

Figure 2. Experimental setup for the isolated blood vessel perfusion system. Representative schematic illustrating the isolated blood vessel perfusion system used to assess vascular responses to perfusion with hemoglobin-based oxygen carriers (HBOCs). (A) Photograph of the isolated vessel chamber setup with a mounted rabbit arteriolar vessel segment. (B) Microscopic image of a cannulated and pressurized arteriole vessel segment. New Zealand white rabbit arterioles vessel segments were isolated, cannulated, and mounted in a temperature-controlled vessel chamber maintained at physiological temperature (37 °C). Vessels were perfused with HBOC and fresh whole blood mixtures at varying flow rates, maintaining a constant mean pressure of 60 mmHg. Blood vessel diameter changes were continuously recorded using video microscopy coupled with a video dimension analyzer for real-time vascular response measurement.

https://doi.org/10.1021/acsabm.6c00900
ACS Appl. Bio Mater. XXXX, XXX, XXX–XXX

Systemic Variables and Blood Chemistry

The mean arterial pressure (MAP) and heart rate (HR) were continuously monitored throughout the experiment using the carotid artery catheter connected to a pressure transducer and data acquisition system (MP150, Biopac Systems, Santa Barbara, CA). Hematocrit (Hct) was determined by centrifugation of arterial blood collected in heparinized capillary tubes. The total hemoglobin (tHb) concentration was measured from a single drop of arterial blood using a portable spectrophotometer (B-Hemoglobin, HemoCue, Stockholm, Sweden). Additional arterial blood samples (50 μL) were collected in heparinized glass capillaries and immediately analyzed for blood gas and metabolic parameters, including pO_2, pCO_2, pH, electrolytes, and lactate, using a blood gas analyzer (ABL90 FLEX, Radiometer America, Brea, CA).

Microvascular Experimental Setup

For intravital microscopy, conscious hamsters were placed in a custom restraining tube that allowed the dorsal window chamber to extend through a longitudinal opening and be secured on the microscope stage. Animals were allowed to acclimate to the restraint for 30 min before data acquisition. Images of the exposed microcirculation were obtained using a transillumination intravital microscope (BX51WI, Olympus, New Hyde Park, NY) equipped with a CCD camera (COHU 4815, San Diego, CA). The video signal was recorded and displayed in real time for subsequent analysis. Microvascular observations were performed using a 40× water-immersion objective (LUMPFL-WIR, numerical aperture 0.8, Olympus). The same predefined vascular regions were imaged throughout the experiment to enable direct comparisons with each animal's baseline measurements.

Microhemodynamics

Arteriolar and venular blood flow velocities were measured online by using the photodiode cross-correlation method[18] (Photo Diode/Velocity Tracker Model 102B, Vista Electronics, San Diego, CA). A set of two fiber optics coupled to two photodiodes are placed on the CCD camera, which is attached to the camera port of the inverted microscope allowing for the image from the microscope to be projected onto the photodiodes and the camera sensor at the same time. The measured centerline velocity (V) was corrected according to blood vessel size to obtain the mean RBC velocity.[19] A video image-shearing method was used to measure the blood vessel diameter (D).[20] The vessel diameter was measured using the video image-shearing technique, which takes advantage of the linear response of the imaging system to provide high spatial resolution. Under the magnification used in this study, the measurement precision was approximately 0.2 μm for a vessel with a diameter of 10 μm occupying half of the video image width. Microvascular blood flow (Q) was calculated using the measured mean RBC velocity (V) and vessel diameter (D) according to the equation $Q = \pi V(D/2)^2$.

To minimize temporal variability in the microcirculation, the vessel diameter and RBC velocity were recorded within the first 10 min of each imaging session. Before experimental measurements, the microvascular network was mapped and the same arterioles and venules were identified for repeated analysis throughout the study. Each vessel was analyzed independently. The vessel type was determined from the direction of RBC flow, with arterioles identified by flow from feeding vessels toward daughter branches and venules identified by flow from daughter branches into collecting vessels.

For analysis, vessels were categorized into three groups according to their diameter: arterioles <60 μm, arterioles >60 μm, and venules ranging from 20 to 80 μm. This classification was selected because vascular reactivity differs across vessel classes. Larger feeding arterioles (>60 μm) typically undergo relatively small changes in diameter (<20%), whereas smaller resistance arterioles (<60 μm), including arcading, transverse, and terminal arterioles, exhibit substantially greater vasomotor responses and therefore play a more prominent role in regulating microvascular blood flow.[21] Venules are known for their compliance in response to pressure changes influenced by arteriole blood flow, and this grouping was intended to simplify the data analysis since the change is uniform across blood vessel sizes.

Functional Capillary Density (FCD)

Functional capillary density (FCD) was assessed 30 min following infusion as a measure of nutritive microvascular perfusion. A capillary was considered functional if at least one red blood cell (RBC) traversed the vessel during a 45 s observation period. Approximately 10 adjacent microscopic fields (0.05 mm^2 per field; total analyzed area ≈ 0.5 mm^2) were evaluated within the window chamber. At baseline, each field typically contained two to eight perfused capillary segments. Capillaries were identified as microvessels permitting single-file RBC passage. FCD was calculated by summing the length of all RBC-perfused capillary segments within each field and normalizing this value to the corresponding tissue area (cm^{-1}). Changes in FCD are reported relative to each animal's baseline measurement, with reductions reflecting diminished tissue capillary perfusion.[22,23]

Microvascular Vascular Resistance and Wall Shear Rate Calculation

Microvascular vascular resistance (R) was calculated 30 min after hypervolemic top-load infusion as the ratio of mean arterial pressure (MAP; ΔP) to microvascular blood flow (Q), where $R = \Delta P/Q$. MAP was continuously recorded via carotid artery catheterization connected to a pressure transducer (MP150, Biopac Systems, Santa Barbara, CA). Microvascular blood flow (Q) was calculated using the measured RBC velocity and blood vessel diameter. Vascular resistance values were expressed as ratios relative to each blood vessel's baseline measurement to account for interanimal variability. Analyses were performed separately for arterioles <60 μm, arterioles >60 μm, and venules (20–80 μm diameter).

The wall shear rate (WSR) was calculated 30 min after hypervolemic top-load infusion in arterioles <60 μm, arterioles >60 μm, and venules (20–80 μm in diameter) using the equation WSR = 8 V/D, where V represents the mean red blood cell (RBC) velocity and D represents the vessel diameter. WSR values were expressed as ratios relative to each blood vessel's baseline measurement to account for interanimal variability.

Data Analysis

Statistical analyses were performed using GraphPad Prism 10 (GraphPad Software, San Diego, CA, USA). Statistical significance was defined as $P < 0.05$. The ex vivo isolated arteriole experiments included 18 independent vessel segments per experimental condition, and results are reported as means ± standard deviation (SD). Differences among treatment groups were evaluated using one-way analysis of variance (ANOVA) followed by Tukey's multiple-comparison post hoc test, an approach commonly employed for biological datasets with multiple treatment groups.[24] Data from the in vivo microvascular studies are also presented as means ± SD. Longitudinal measurements obtained within the same experimental group were analyzed using repeated-measures ANOVA. When data did not satisfy the assumptions of normality, the nonparametric Kruskal–Wallis test was used, followed by Dunn's multiple-comparison test where appropriate. Comparisons involving two independent variables (e.g., HBOC formulation and time) were evaluated using two-way ANOVA with Bonferroni's post hoc correction. Comparisons between experimental groups were performed using two-way ANOVA, considering HBOC formulation and time as independent variables, followed by Bonferroni post hoc multiple-comparison tests, consistent with previously reported methodologies.[25,26] Microhemodynamic measurements are presented as box-and-whisker plots to illustrate the distribution of the data. The central line within each box represents the median, while the lower and upper boundaries correspond to the 25th and 75th percentiles, respectively. Whiskers extend to the 5th and 95th percentiles. Vascular resistance is presented separately as means ± standard deviation using bar graphs.

https://doi.org/10.1021/acsabm.6c00900
ACS Appl. Bio Mater. XXXX, XXX, XXX–XXX

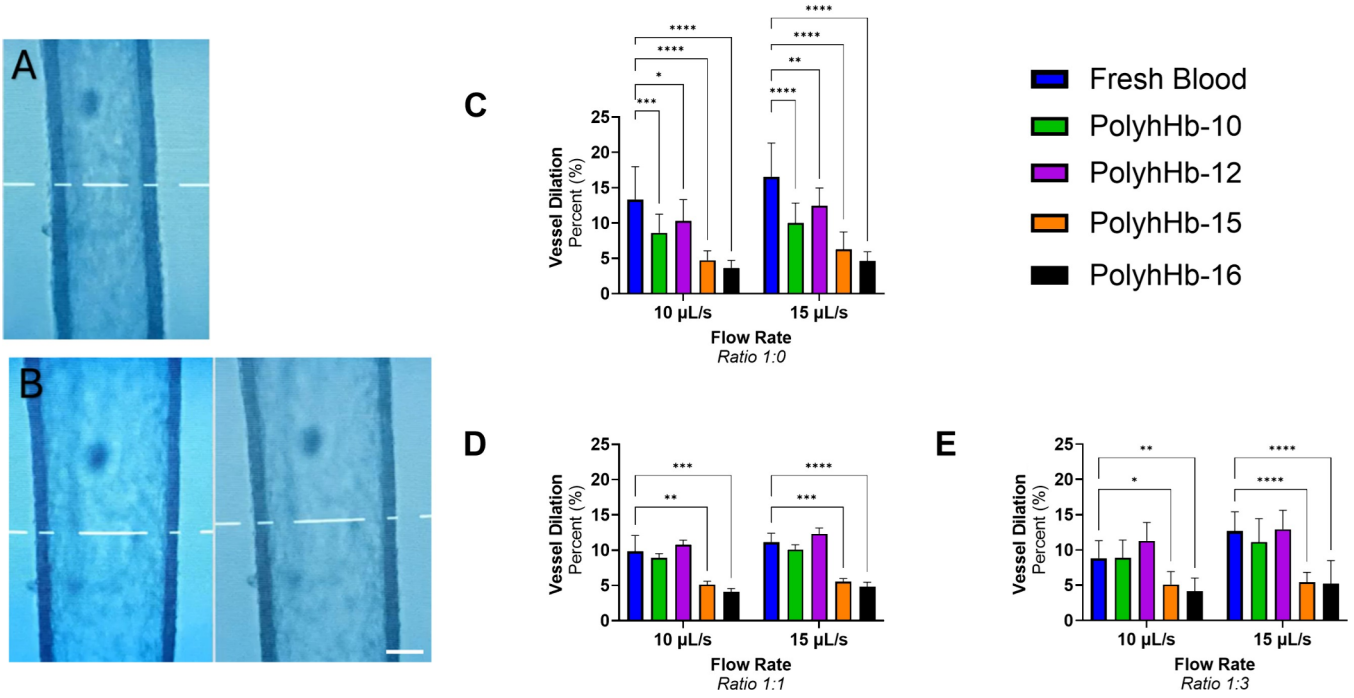

Figure 3. Flow-mediated dilation (FMD) in isolated arterioles perfused with polymerized human hemoglobin formulations. Representative microscopic images demonstrating arteriole diameter changes from (A) baseline conditions to (B) a vasodilatory state following flow-mediated stimulation. White reference lines indicate the baseline vessel diameter and subsequent vessel expansion, representative of endothelium-dependent dilation. Images were acquired using video microscopy and analyzed using a real-time vessel analyzer. Scale bar = 100 µm. Quantification of blood vessel dilation (%) in isolated mesenteric arterioles excised from New Zealand white rabbits and perfused with fresh whole blood mixed with different polymerized human hemoglobin formulations (PolyhHb-10, PolyhHb-12, PolyhHb-15, and PolyhHb-16) at hemoglobin solution-to-whole blood volume:volume ratios of (C) 1:0, (D) 1:1, and (E) 1:3. Blood vessel responses were measured at flow rates of 10 and 15 µL/s while maintaining a mean perfusion pressure of 60 mmHg to evaluate the effects of PolyhHb molecular size on flow-mediated dilation. Each condition included 18 independent blood vessels per flow rate and mixing ratio, with an average baseline vessel diameter of 398 ± 66 µm. Data are presented as the mean ± standard deviation. Statistical comparisons were performed relative to PolyhHb-12, with $P < 0.05$ (*), $P < 0.01$(**), $P < 0.001$ (***), and $P < 0.0001$ (****).

To account for interanimal variability, vascular resistance and all microhemodynamic parameters were normalized to their respective baseline values and expressed as fold changes. A value of 1.0 indicates no change from baseline, whereas values above or below 1.0 represent proportional increases or decreases, respectively (e.g., a value of 1.5 corresponds to a 50% increase relative to baseline). Because the same blood vessels and capillary fields were evaluated before and after treatment, each vessel served as its own internal control, enabling paired comparisons and improving statistical robustness despite relatively small sample sizes.

Sample size was determined by an a priori power analysis using analysis of variance (ANOVA). Assuming a significance level (α) of 0.05 and a statistical power of 0.90, the analysis indicated that a minimum of 15 microvessels per experimental group was required to detect a statistically significant difference.

RESULTS

Flow Dependency in Isolated Blood Vessels

The flow-mediated dilation (FMD) responses in isolated blood vessels perfused with varying volume:volume ratios (1:0, 1:1, and 1:3) of different PolyhHb formulations are presented in Figure 3. All ratios and flow rates are expressed as the percent change from the blood vessel's initial diameter recorded with PSS initially. Eighteen ($n = 18$) blood vessels per flow rate per ratio were evaluated, with an average baseline diameter of 398 ± 66 µm.

At a perfusion ratio of 1:0, fresh blood produced the greatest overall vasodilation across flow rates, serving as the physiologic benchmark. Among the HBOCs, PolyhHb-12 most closely preserved fresh blood-mediated dilation; however, in comparison to fresh blood, it was significantly lower, $P < 0.05$ at 10 µL/s and $P < 0.01$ at 15 µL/s, indicating the superiority of fresh blood (an anticipated result). Furthermore, when comparing fresh blood to PolyhHb-10 ($P < 0.001$ at 10 µL/s and $P < 0.0001$ at 15 µL/s), PolyhHb-15 ($P < 0.0001$ at 10 µL/s and $P < 0.0001$ at 15 µL/s,) and PolyhHb-16 ($P < 0.0001$ at 10 µL/s and $P < 0.0001$ at 15 µL/s,) all solutions showed even further inferiority to fresh blood. PolyhHb-15 and PolyhHb-16 exhibited the most attenuated dilation relative to fresh blood.

At a 1:1 ratio (HBOC:fresh whole blood), vasodilatory responses follow similar trends as the 1:0 ratio. PolyhHb-12 again provided the closest response to fresh blood-induced flow-mediated dilation (FMD). While differences between PolyhHb-12 and PolyhHb-10 were modest and both did not show significant differences when compared to fresh blood at either flow rate, PolyhHb-12 maintained greater percent dilation. However, PolyhHb-15 ($P < 0.01$ at 10 µL/s and $P < 0.001$ at 15 µL/s) and PolyhHb-16 ($P < 0.001$ at 10 µL/s and $P < 0.0001$ at 15 µL/s) both demonstrated a significant reduction in FMD compared to fresh blood with PolyhHb-16 having the lowest percentage of dilation out of all groups. Larger polymers continued to demonstrate reduced

https://doi.org/10.1021/acsabm.6c00900
ACS Appl. Bio Mater. XXXX, XXX, XXX–XXX

vasodilatory capacity relative to fresh blood, particularly at higher shear rates.

At a 1:3 ratio, PolyhHb-12 continued to exhibit the strongest preservation of FMD among all HBOCs, demonstrating greater vascular response compared to its HBOC counterparts. Similarly as it was noticed with 1:1 ratios, PolyhHb-12 and PolyhHb-10 showed no significant differences when compared to fresh blood, but just as before, PolyhHb-12 exhibits greater FMD than PolyhHb-10. Also, just as before, larger polymers show progressively diminished FMD compared to fresh blood (PolyhHb-15 $P < 0.05$ at 10 μL/s and $P < 0.0001$ at 15 μL/s, PolyhHb-16 $P < 0.01$ at 10 μL/s and $P < 0.0001$ at 15 μL/s).

Acetylcholine Infusion Isolated Blood Vessels

NO-mediated dilation following ACh infusion at a constant flow rate of 3 μL/s is presented in Figure 4 across HBOC-to-whole blood volume:volume ratios (1:0, 1:1, and 1:3). Fresh blood served as a physiological reference and demonstrated the greatest vasodilatory response under all ratio conditions. Compared to all HBOC groups, fresh blood FMD was significantly greater ($P < 0.0001$). However, this is expected as the fresh blood's RBC membrane prevents NO scavenging; in contrast to the HBOC groups with freely exposed hemoglobin, NO scavenging is inevitable. Nevertheless, valuable information regarding NO scavenging as a function of HBOC size is produced.

At the 1:0 ratio (HBOC alone), vasodilation was attenuated compared with fresh blood across all HBOC formulations. Among HBOCs, PolyhHb-12 produced the largest FMD. At the 1:1 ratio, vasodilatory responses improved modestly compared with the 1:0 condition and PolyhHb-12 again exhibited the strongest FMD. At the 1:3 ratio, PolyhHb-12 maintained the highest FMD response, but PolyhHb-10 showed a substantial improvement compared to its FMD at the other two ratios. The larger HBOC (PolyhHb-15 and PolyhHb-16) continued to struggle.

Microvascular Hemodynamics

Relative changes in microvascular diameter (A−C) and relative changes in microvascular blood flow (D−F) measured 30 min after hypervolemic infusion are presented Figure 5. HSA (10% w/v) was included as a positive control to control establish the effects of using a protein of similar molecular weight to hHb (~66 kDa) but without NO scavenging activity, allowing separation of size/volume effects from Hb-specific vasoactivity.

In arterioles <60 μm, the microhemodynamic diameter for hHb demonstrated significant vasoconstriction when compared to HSA ($P < 0.01$), PolyhHb-12 ($P < 0.0001$), PolyhHb-15 ($P < 0.0001$), and PolyhHb-16 ($P < 0001$) but no significant changes when compared to PolyhHb-10. Furthermore, when comparing to baseline HSA, PolyhHb-10 and PolyhHb-16 had no significance, but hHb ($P < 0.05$) had the largest drop in microvascular diameter. Also, PolyhHb-12 noticed significant vasodilation compared to baseline ($P < 0.05$). Furthermore, the microhemodynamic blood flow in arterioles <60 μm illustrated a significant increase in PolyhHb-12 ($P < 0.0001$) when compared to hHb, but PolyhHb-10, PolyhHb-15, and PolyhHb-16 showed no significant differences when compared to hHb. When comparing directly to baseline hHb ($P < 0.05$) illustrated a significant drop in microhemodynamic blood flow, PolyhHb-12 illustrated a significant rise ($P < 0.05$) in microhemodynamic blood flow, and PolyhHb-10, PolyhHb-15, and PolyhHb-16 showed no significant changes.

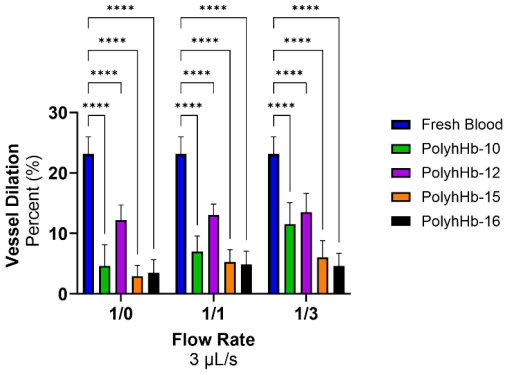

Figure 4. Acetylcholine (Ach) infused isolated arterioles. A small dose of Ach (1 μmol/L) was mixed with various hemoglobin-based oxygen carriers (HBOC) and New Zealand white rabbit whole blood in three different volume:volume ratios of 1:0, 1:1, and 1:3 of HBOC to whole blood. This mixture was used to perfuse 18 individual isolated blood vessels per group at each ratio to assess the percentage of maximum vasodilation at a flow rate of 3 μL/s (and at a mean prefusion pressure of 60 mmHg)). The average blood vessel diameter was 398 ± 66 μm. The Ach-induced vasodilation was performed to evaluate the NO scavenging capacity of each perfusate solution. The data are presented as the mean ± standard error of the mean. Asterisks denote comparisons to fresh blood * ($P < 0.05$), ** ($P < 0.01$), *** ($P < 0.001$), and **** ($P < 0.0001$). The analysis focused on the significance related to the ratio of HBOC to fresh blood only.

In arterioles >60 μm, the microhemodynamic diameter for hHb demonstrated significant vasoconstriction when compared to HSA ($P < 0.0001$), PolyhHb-12 ($P < 0.0001$), PolyhHb-15 ($P < 0.0001$), PolyhHb-16 ($P < 0001$) but no significant changes when compared to PolyhHb-10. When comparing to baseline, hHb ($P < 0.05$) illustrated significant vasoconstriction, and none of the HBOC variants had significant changes compared to baseline. Furthermore, the microhemodynamic blood flow in arterioles >60 μm illustrated no significant differences compared to hHb. When compared to baseline, hHb ($P < 0.05$) was significantly reduced and no other experimental group was significant to baseline.

In venules (20–80 μm), the microhemodynamic diameter for hHb demonstrated significant vasoconstriction compared to HSA ($P < 0.01$) and no other group showed significant changes when compared to hHb. When compared to baseline, no significant changes were seen. Additionally, the microhemodynamic blood flow in venules (20–80 μm) illustrated a significant rise in blood flow with HSA ($P < 0.01$) when compared to hHb no other significant changes were noticed. When compared to baseline, hHb showed a significant drop ($P < 0.05$) and no other group had any significant changes.

Functional Capillary Density

Changes in FCD at 30 min after infusion with different HBOCs relative to baseline are presented in Figure 6. All HBOC formulations exhibited a significant reduction in FCD compared to baseline ($P < 0.05$), with HSA preserving and improving to FCD. When comparing directly to hHb, all groups showed significant improvement except for PolyhHb-10, HSA ($P < 0.0001$), PolyhHb-12 ($P < 0.01$), PolyhHb-15 ($P < 0.01$), and PolyhHb-16 ($P < 0.01$). This indicates an overall impairment in capillary perfusion postinfusion when using HBOCs depending on size.

https://doi.org/10.1021/acsabm.6c00900
ACS Appl. Bio Mater. XXXX, XXX, XXX−XXX

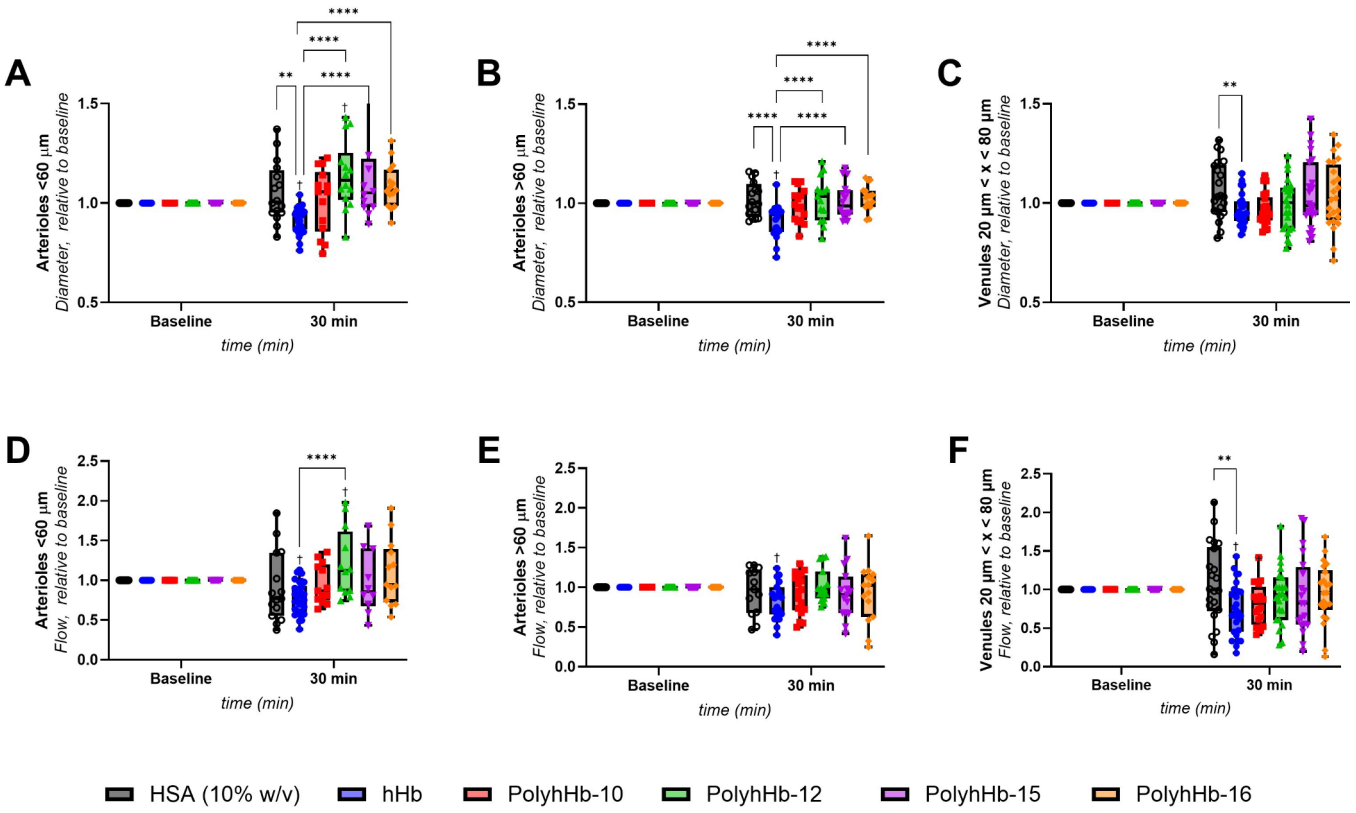

Figure 5. In vivo microvascular diameter and flow responses following HBOC infusion. Relative changes in microvascular diameter (A–C) and blood flow (D–F) were assessed 30 min after hypovolemic infusion of human serum albumin (HSA, 10% w/v), human hemoglobin (hHb), or polymerized hHb formulations of increasing molecular size (PolyhHb-10, PolyhHb-12, PolyhHb-15, and PolyhHb-16) in Golden Syrian hamsters instrumented with a dorsal window chamber. Blood vessel diameters and blood flows are shown for arterioles >60 µm (A, D), arterioles <60 µm (B, E), and venules between 20–80 µm (C, F), normalized to baseline (dashed line). The average baseline flow rates were 4.0 ± 1.9 nL/s for arterioles <60 µm, 23.3 ± 2.6 nL/s for arterioles >60 µm, and 2.04 ± 0.47 nL/s for venules, reflecting distinct microvascular shear environments. HSA was administered at the same mass concentration (10 g/dL) as all PolyhHb solutions and serves as a nonoxygen-carrying, non-NO-scavenging colloid control. Native hHb, despite having a molecular weight comparable to HSA, produced greater vasoconstriction and flow reduction, particularly in resistance arterioles, consistent with Hb-mediated nitric oxide (NO) scavenging under low-flow conditions. Increasing PolyhHb molecular size progressively preserved the arteriolar diameter and microvascular flow, with PolyhHb-12, PolyhHb-15, and PolyhHb-16 demonstrating significantly improved microvascular stability relative to hHb. Data are presented as box-and-whisker plots. Each group includes measurements from 15 independent vessels derived equally from six animals. Symbols denote statistical significance compared to baseline (†) and hHb (*$P < 0.05$, **$P < 0.01$, ***$P < 0.001$, and ****$P < 0.0001$).

Size-Dependent Changes in Microvascular Vascular Resistance

Relative microvascular vascular resistance ($R = \Delta P/Q$), normalized to baseline, measured 30 min following hypervolemic top-load infusion across arterioles <60 µm, arterioles >60 µm, and venules (20–80 µm) are presented in Figure 7.

In all sized arterioles (<60 and >60 µm) and venules (20–80 µm), hHb produced the greatest increase in vascular resistance relative to baseline ($P < 0.05$). When comparing between groups, PolyhHb-12 illustrated a significant drop in vascular resistance compared to hHb ($P < 0.0001$ in arterioles <60 µm and $P < 0.01$ in arterioles >60 µm). No other group illustrated any significant changes to baseline or compared to hHb.

Microvascular Wall Shear Rate following HBOC Infusion

Relative changes in the wall shear rate (WSR), normalized to baseline, measured 30 min after hypervolemic infusion across arterioles <60 µm, arterioles >60 µm, and venules (20–80 µm) are shown in Figure S3. No significant differences were observed when compared to hHb or to baseline. These results are anticipated as the hypovolemic infusion does not have enough volume to cause changes to hemorheology profiles.

Systemic Hemodynamics after Infusion In Vivo

Relative changes in MAP and HR 30 min following hypervolemic infusion, normalized to baseline, are shown in Figure S2. Human Hb produced the greatest increase in MAP ($P <$ 0,05) and the largest reduction in HR ($P < 0.05$) compared to baseline. PolyhHb-10 demonstrated a significant rise in MAP ($P < 0.05$) and a significant decline in HR ($P < 0.05$), whereas PolyhHb-12, PolyhHb-15, and PolyhHb-16 maintained MAP and HR values closer to baseline. HSA remained near baseline for both MAP and HR, increasing our speculation that the hypertensive and bradycardic responses are primarily driven by Hb-specific NO scavenging rather than small-protein infusion alone.

https://doi.org/10.1021/acsabm.6c00900
ACS Appl. Bio Mater. XXXX, XXX, XXX–XXX

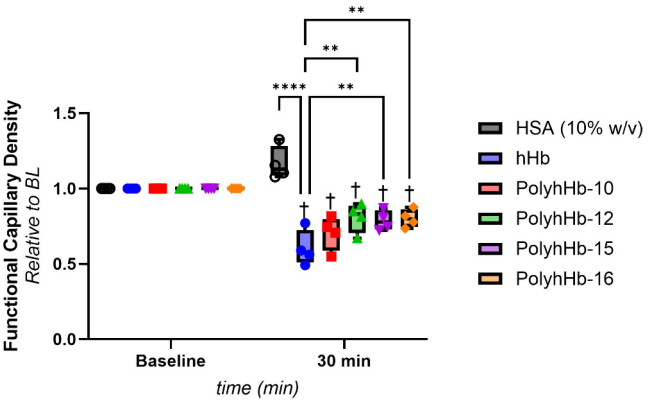

Figure 6. Functional capillary density (fcd) following hemoglobin-based oxygen carrier (HBOC) infusion. The FCD was assessed 30 min after hypovolemic infusion of human serum albumin (HSA, 10% w/v), acellular human Hb (hHb), or PolyhHb formulations of increasing molecular size (PolyhHb-10, PolyhHb-12, PolyhHb-15, and PolyhHb-16) in Golden Syrian hamsters instrumented with dorsal window chambers. Functional capillaries were defined as single capillaries segments in which at least one red blood cell (RBC) flowed within a 45 s interval. The FCD per animal is evaluated across approximately 10–12 consecutive independent microscopic fields, and the same fields are studied each time. Values are normalized to baseline to account for interanimal variability per field. Infusion with hHb resulted in a marked reduction in FCD, whereas increasing PolyhHb size progressively preserved capillary perfusion, with PolyhHb-16 demonstrating the greatest preservation of FCD. Data represent measurements from six animals per group. Symbols denote statistical significance compared to baseline (†) and hHb (**$P < 0.01$, ***$P < 0.001$, and ****$P < 0.0001$).

Blood Gas, Hematological, and Systemic Hemodynamic Responses to HBOC Infusion

Blood gas measurements and systemic variables at baseline and after infusion of HBOCs are summarized in Table S1. Hematocrit (Hct), total hemoglobin (tHb), arterial partial pressure of oxygen (pO_2), partial pressure of carbon dioxide (pCO_2), and pH levels remained relatively consistent across all experimental groups, with no significant deviations observed postinfusion.

■ DISCUSSION

We hypothesized that the PolyhHb polymer architecture/molecular size represents a critical, yet underexplored, determinant of NO scavenging and vascular compatibility. The results of this study are consistent with this hypothesis and suggest that controlled increases in polymer size are associated with systematic changes in vascular behavior across multiple scales, including arteriolar resistance, wall shear rate, blood vessel diameter, blood flow, and FCD. Notably, these effects were observed despite preserved intrinsic NO scavenging capacity across all PolyhHb formulations, suggesting that spatial distribution and near-wall transport, rather than chemically modulating NO scavenging,[27,28] may play a dominant role in shaping the effective vascular response to HBOCs.

In the isolated blood vessel perfusion model, PolyhHb molecular size was associated with distinct differences in flow-mediated dilation reactivity under controlled hydrodynamic conditions. Fresh whole blood consistently produced the greatest degree of flow-mediated dilation. Across all HBOC-to-blood volume:volume ratios, PolyhHb reduced vasodilation relative to fresh blood; however, the extent of this attenuation changed with polymer molecular size. In particular, PolyhHb-12 tended to preserve blood flow-mediated dilation compared to smaller or larger PolyhHb formulations, suggesting that intermediate polymer architectures may be more favorable for maintaining endothelial shear stress responsiveness under blood flow conditions. The driving force for this phenomenon lies in what we believe to be the Segre−Silberberg effect, in which PolyhHb flowing through a tube migrates to a specific equilibrium position between the center and away from the walls and the endothelium.[29,30]

Mechanistically, our findings suggest that HBOC molecular size governs vascular responses through a balance between transport phenomena and rheological effects rather than only changes in the intrinsic chemistry of nitric oxide (NO) scavenging. Smaller HBOCs remain more uniformly distributed throughout the plasma and readily diffuse toward the endothelial surface, increasing the probability of intercepting endothelial-derived NO and promoting vasoconstriction. As molecular size increases, hydrodynamic lift forces and exclusion from the cell-free layer may increase the average separation between PolyhHb and the endothelium, thereby reducing the effective NO scavenging while preserving endothelial-dependent vasodilatory signals. However, further increases in polymer size might increase plasma viscosity, intermolecular interactions, and macromolecular crowding, partially offset these transport advantages, and limit blood flow and the hemodynamic improvements on vascular function. Consequently, PolyhHb-12 appears to occupy an optimal transport regime in which endothelial NO signaling, microvascular perfusion, and systemic hemodynamic stability are best balanced. This idea is rooted on similar studies that show how higher plasma viscosity reduced erythrocyte cell-free layer thickness and increased wall shear stress, thereby altering erythrocyte column hydrodynamics and shear stress on the vascular endothelium and affecting microvascular perfusion and consequently oxygen delivery.[27]

To further distinguish transport-related effects from changes in NO production, an ACh-mediated dilation experiments were performed. In healthy blood vessels, ACh acts as a potent vasodilator by triggering the release of NO independently of flow; these experiments provided an opportunity to assess the effects of PolyhHbs of difference sizes on endothelial NO-mediated dilation. Under flow conditions, the ACh-mediated dilation was best preserved in blood vessels perfused with PolyhHb-12, whereas larger formulations, including PolyhHb-15 and PolyhHb-16, exhibited blunted responses. When considered together with the flow-mediated dilation, these findings support the possibility that the effective rate of NO scavenging is influenced by the proximity of acellular Hb to the endothelial NO source, rather than by differences in NO synthesis or intrinsic scavenging chemistry.

To further strengthen our hypothesis surrounding acellular Hb molecular size, we moved toward in vivo experimentation, and our results further confirm the molecular size-dependent framework. To establish suitable comparison and better understandings of PolyhHb molecular size, we used HSA at equal concentrations as a positive control. HSA represents a molecule of similar size to acellular Hb at 66 kDa but does not scavenge NO.[31,32] Following hypervolemic top-load infusion, PolyhHb molecular size was associated with differences in microvascular resistance, wall shear rate, blood vessel diameter, and blood flow

https://doi.org/10.1021/acsabm.6c00900
ACS Appl. Bio Mater. XXXX, XXX, XXX−XXX

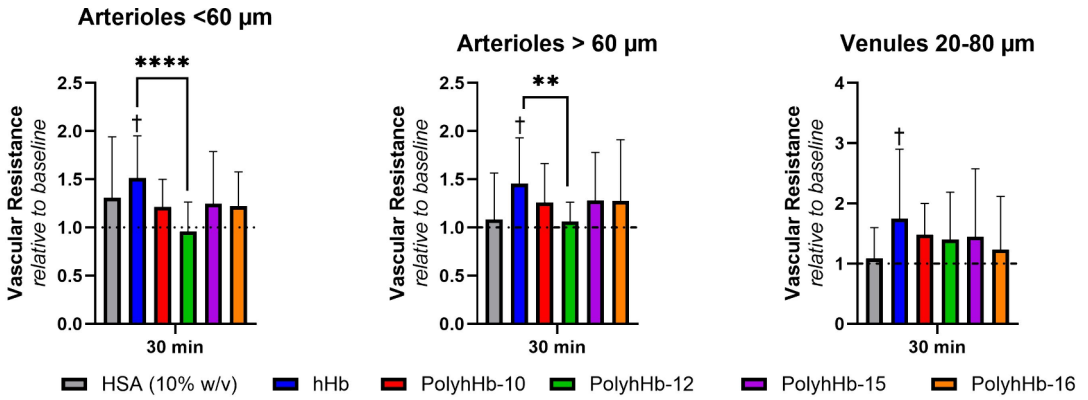

Figure 7. Size-dependent changes in microvascular vascular resistance following hemoglobin-based oxygen carrier (HBOC) infusion. Relative vascular resistance, normalized to baseline, measured 30 min after infusion in small arterioles <60 μm, mid-size arterioles >60 μm, and small venules (20–80 μm diameter). Vascular resistance was calculated as $R = \Delta P/Q$, where ΔP is the mean arterial pressure (MAP) and Q is the microvascular blood flow, and expressed as a ratio relative to each vessel's baseline value. Resistance responses are shown for human serum albumin (HSA, 10% w/v), acellular human Hb (hHb), and polymerized hHb formulations (PolyhHb-10, PolyhHb-12, PolyhHb-15, and PolyhHb-16). Smaller arterioles (<60 μm), which are highly sensitive to NO regulation, exhibited significantly lower resistance with PolyhHb-12 compared to other polymer sizes, indicating improved microvascular compatibility. Larger arterioles (>60 μm) showed modest but significant size-dependent differences, while venules demonstrated minimal resistance changes across groups. Data are presented as means ± SD. Dagger symbols (†) denote significant differences relative to baseline, while asterisks indicate intergroup comparisons ($^*P < 0.05$, $^{**}P < 0.01$, and $^{****}P < 0.0001$).

in a blood vessel class-dependent manner and FCD. Small arterioles (<60 μm), which serve as primary resistance vessels and are highly sensitive to NO scavenging and are responsible for vascular resistance and an oxygen delivery. Acellular Hb produced the largest increase in resistance, whereas PolyhHb formulations attenuated resistance to varying degrees, with PolyhHb-12 generally exhibiting the most favorable profile. Larger polymers partially reduced resistance but did not consistently reproduce resistant below PolyhHb-12, suggesting that excessive polymer size may introduce additional transport-related constraints.

These resistance changes were accompanied by corresponding alterations in the wall shear rate and wall shear stress. In small arterioles, acellular Hb was associated with increased shear rates, consistent with vasoconstriction and elevated blood flow velocity. Increasing the PolyhHb molecular size tended to reduce the wall shear rate, with the largest reductions observed for PolyhHb-12, PolyhHb-15, and PolyhHb-16. Because the wall shear rate determines the wall shear stress and modulates endothelial mechanotransduction and endothelial NO production, these findings suggest that polymer molecular size might influence the mechanical environment sensed by the endothelium. In contrast, venular shear rates remained largely unchanged, indicating that HBOC-induced hemodynamic effects are concentrated within NO-sensitive resistance vessels.

Consistent with these upstream effects, PolyhHb-12 was associated with superior preservation of the arteriolar diameter and blood flow across vessel classes compared with acellular Hb and smaller polymers. At the capillary level, FCD decreased markedly following acellular Hb infusion but was preserved to varying degrees by PolyhHb. Larger polymers (PolyhHb-12, PolyhHb-15, and PolyhHb-16) demonstrated similar capillary perfusion levels. However, PolyhHb-12 appeared to achieve a more balanced hemodynamic profile, preserving capillary perfusion while maintaining arteriolar resistance and shear stress.

Taken together, these findings suggest that vascular compatibility of HBOCs may depend on polymer molecular size and its near-wall displacement to prevent unwanted NO scavenging. Intermediate polymer sizes, such as PolyhHb-12, may occupy a favorable regime in which axial displacement, shear regulation, and NO signaling are balanced, highlighting PolyhHb molecular size as an important design consideration for next-generation HBOCs.

CONCLUSIONS

In conclusion, our comprehensive evaluation demonstrates that PolyhHb molecular size is a critical determinant of vascular function, systemic hemodynamics, and microvascular blood flow. Among the formulations evaluated, PolyhHb-12 provided the most favorable balance between preserving endothelial function, maintaining microvascular blood flow, and minimizing adverse vascular responses, supporting its potential as a next-generation HBOC for resuscitation from hemorrhagic shock when blood products are unavailable or in austere conditions. Although our findings support a transport-based mechanism linking PolyhHb molecular size with NO scavenging, bioavailability, and vascular compatibility, these mechanisms were inferred from physiological responses and were not directly measured. Future studies will focus on directly characterizing PolyhHb molecular size effects on transport within the microcirculation, quantifying its interaction with endothelial NO, and evaluating long-term safety and efficacy in clinically relevant models of hemorrhagic shock to facilitate potential translation toward clinical application.

ASSOCIATED CONTENT

Supporting Information

The Supporting Information is available free of charge at https://pubs.acs.org/doi/10.1021/acsabm.6c00900.

https://doi.org/10.1021/acsabm.6c00900
ACS Appl. Bio Mater. XXXX, XXX, XXX–XXX

(Figure S1) Experimental timeline and setup, (Figure S2) hemodynamic responses following HBOC infusion, (Figure S3) relative wall shear rate in microvessels, and (Table S1) blood gas and systemic measurements (DOCX)

AUTHOR INFORMATION

Corresponding Author

Pedro Cabrales – *Department of Bioengineering, University of California San Diego, La Jolla, California 92093-0021, United States;* orcid.org/0000-0002-8794-2839; Email: pcabrales@ucsd.edu

Authors

Carlos Munoz – *Department of Bioengineering, University of California San Diego, La Jolla, California 92093-0021, United States*

Daniela Lucas – *Department of Bioengineering, University of California San Diego, La Jolla, California 92093-0021, United States;* orcid.org/0009-0005-0101-4628

Jacinda Martinez – *Department of Bioengineering, University of California San Diego, La Jolla, California 92093-0021, United States*

Nathaniel Ung – *Department of Bioengineering, University of California San Diego, La Jolla, California 92093-0021, United States;* orcid.org/0000-0003-2609-3789

Mohd Asim Khan – *William G. Lowrie Department of Chemical and Biomolecular Engineering, The Ohio State University, Columbus, Ohio 43210-1132, United States;* orcid.org/0000-0002-4698-2332

Tanmay Salvi – *William G. Lowrie Department of Chemical and Biomolecular Engineering, The Ohio State University, Columbus, Ohio 43210-1132, United States;* orcid.org/0000-0002-2538-3920

Griffin J. Beyer – *William G. Lowrie Department of Chemical and Biomolecular Engineering, The Ohio State University, Columbus, Ohio 43210-1132, United States;* orcid.org/0009-0009-6367-3046

Andre F. Palmer – *William G. Lowrie Department of Chemical and Biomolecular Engineering, The Ohio State University, Columbus, Ohio 43210-1132, United States*

Complete contact information is available at: https://pubs.acs.org/doi/10.1021/acsabm.6c00900

Author Contributions

C.M. and J.M. wrote the main manuscript text and prepared the figures; C.M., J.M., N.U., and D.L. performed the experiments and analyzed the data; C.M., J.M., N.U., D.L., M.A.K., T.S., G.J.B., A.F.P., and P.C. reviewed and revised the manuscript; and all authors contributed to the design and implementation of the experiment.

Notes

All images, artwork, and photographs appearing in the manuscript, including graphics, were created by the authors of this manuscript. The authors declare no competing financial interest.

ACKNOWLEDGMENTS

The authors would like to acknowledge Cynthia Walser for performing the hamster window chamber surgeries and catheterizations, as well as for managing the purchasing and housing logistics essential to this study.

REFERENCES

(1) Alarhayem, A. Q.; Myers, J. G.; Dent, D.; Liao, L.; Muir, M.; Mueller, D.; Nicholson, S.; Cestero, R.; Johnson, M. C.; Stewart, R.; O'Keefe, G.; Eastridge, B. J. Time Is the Enemy: Mortality in Trauma Patients with Hemorrhage from Torso Injury Occurs Long before the "Golden Hour". *Am. J. Surg.* **2016**, *212* (6), 1101−1105.

(2) Deeb, A.-P.; Guyette, F. X.; Daley, B. J.; Miller, R. S.; Harbrecht, B. G.; Claridge, J. A.; Phelan, H. A.; Eastridge, B. J.; Joseph, B.; Nirula, R.; Vercruysse, G. A.; Sperry, J. L.; Brown, J. B. Time to Early Resuscitative Intervention Association with Mortality in Trauma Patients at Risk for Hemorrhage. *J. Trauma Acute Care Surg.* **2023**, *94* (4), 504−512.

(3) Braverman, M. A.; Smith, A.; Pokorny, D.; Axtman, B.; Shahan, C. P.; Barry, L.; Corral, H.; Jonas, R. B.; Shiels, M.; Schaefer, R. Prehospital Whole Blood Reduces Early Mortality in Patients with Hemorrhagic Shock. *Transfusion* **2021**, *61*, S15−S21.

(4) Hashmi, Z. G.; Jansen, J. O.; Kerby, J. D.; Holcomb, J. B. Nationwide Estimates of the Need for Prehospital Blood Products after Injury. *Transfusion* **2022**, *62* (S1), S203−S210.

(5) Martin, S. M.; Fisher, A. D.; Meledeo, M. A.; Wampler, D.; Nicholson, S. E.; Raczek, K.; April, M. D.; Weymouth, W. L.; Bynum, J.; Schauer, S. G. More Sophisticated than a Drink Cooler or an Old Sphygmomanometer but Still Not Adequate for Prehospital Blood: A Market Review of Commercially Available Equipment for Prehospital Blood Transport and Administration. *Transfusion* **2021**, *61*, S286−S293.

(6) Pokorny, D. M.; Braverman, M. A.; Edmundson, P. M.; Bittenbinder, D. M.; Zhu, C. S.; Winckler, C. J.; Schaefer, R.; McGinity, A. C.; Epley, E.; Eastridge, B. J. The Use of Prehospital Blood Products in the Resuscitation of Trauma Patients: A Review of Prehospital Transfusion Practices and a Description of Our Regional Whole Blood Program in San Antonio, TX. *ISBT Sci. Ser.* **2019**, *14* (3), 332−342.

(7) Hajjaj, O. I.; Modi, D.; Cameron, T.; Barty, R.; Owens, W.; Heddle, N.; Zhang, L.; Thompson, T.; Callum, J. Reducing Blood Product Wastage through the Inter-Hospital Redistribution of near-Outdate Inventory. *Transfusion* **2024**, *64* (7), 1207−1216.

(8) Alayash, A. I. Hemoglobin-Based Blood Substitutes: Oxygen Carriers, Pressor Agents, or Oxidants?. *Nat. Biotechnol.* **1999**, *17* (6), 545−549.

(9) Muller, C. R.; Williams, A. T.; Munoz, C. J.; Eaker, A. M.; Breton, A. N.; Palmer, A. F.; Cabrales, P. Safety Profile of High Molecular Weight Polymerized Hemoglobins. *Transfusion* **2021**, *61* (1), 212−224.

(10) Pimenova, T.; Pereira, C. P.; Schaer, D. J.; Zenobi, R. Characterization of High Molecular Weight Multimeric States of Human Haptoglobin and Hemoglobin-Based Oxygen Carriers by High-Mass MALDI MS. *J. Sep. Sci.* **2009**, *32* (8), 1224−1230.

(11) Greenfield, A.; Lamb, D. R.; Gu, X.; Thangaraju, K.; Setua, S.; Yahya, A.; Vahedi, A.; Khan, M. A.; Wang, Q.; Buehler, P. W.; Palmer, A. F. Biophysical Analysis and Preclinical Pharmacokinetics-Pharmacodynamics of Tangential Flow Filtration Fractionated Polymerized Human Hemoglobin as a Red Blood Cell Substitute. *Biomacromolecules* **2023**, *24* (4), 1855−1870.

(12) Baek, J. H.; Zhou, Y.; Harris, D. R.; Schaer, D. J.; Palmer, A. F.; Buehler, P. W. Down Selection of Polymerized Bovine Hemoglobins for Use as Oxygen Releasing Therapeutics in a Guinea Pig Model. *Toxicol. Sci.* **2012**, *127* (2), 567−581.

(13) Cabrales, P.; Sun, G.; Zhou, Y.; Harris, D. R.; Tsai, A. G.; Intaglietta, M.; Palmer, A. F. Effects of the Molecular Mass of Tense-State Polymerized Bovine Hemoglobin on Blood Pressure and Vasoconstriction. *J. Appl. Physiol.* **2009**, *107* (5), 1548−1558.

(14) Khan, M. A.; Salvi, T.; Beyer, G. J.; Abdalbaqi, A.; Allyn, M.; Bresolin, A.; Palmer, A. F.; on behalf of the CONCERT research

program. Scalable Production and Biophysical Characterization of High-Molecular-Weight Relaxed and Tense Quaternary State Polymerized Human Hemoglobin as Potential Red Blood Cell Substitutes *Biomacromolecules* **2024**, *25* (11), 7334−7348.
(15) Colantuoni, A.; Bertuglia, S.; Intaglietta, M. Quantitation of Rhythmic Diameter Changes in Arterial Microcirculation. *Am. J. Physiol.* **1984**, *246* (4), H508−H517.
(16) Endrich, B.; Asaishi, K.; Götz, A.; Meßmer, K. Technical Report—a New Chamber Technique for Microvascular Studies in Unanesthetized Hamsters. *Res. Exp. Med.* **1980**, *177* (2), 125−134.
(17) Cabrales, P.; Tsai, A. G.; Frangos, J. A.; Intaglietta, M. Role of Endothelial Nitric Oxide in Microvascular Oxygen Delivery and Consumption. *Free Radical Biol. Med.* **2005**, *39* (9), 1229−1237.
(18) Intaglietta, M.; Silverman, N. R.; Tompkins, W. R. Capillary Flow Velocity Measurements in Vivo and in Situ by Television Methods. *Microvasc. Res.* **1975**, *10* (2), 165−179.
(19) Lipowsky, H. H.; Zweifach, B. W. Application of the "Two-Slit" Photometric Technique to the Measurement of Microvascular Volumetric Flow Rates. *Microvasc. Res.* **1978**, *15* (1), 93−101.
(20) Intaglietta, M.; Tompkins, W. R. Microvascular Measurements by Video Image Shearing and Splitting. *Microvasc. Res.* **1973**, *5* (3), 309−312.
(21) Munoz, C. J.; Lucas, A.; Williams, A. T.; Cabrales, P. A Review on Microvascular Hemodynamics: The Control of Blood Flow Distribution and Tissue Oxygenation. *Crit. Care Clin.* **2020**, *36* (2), 293−305.
(22) Cabrales, P.; Tsai, A. G.; Intaglietta, M. Microvascular Pressure and Functional Capillary Density in Extreme Hemodilution with Low- and High-Viscosity Dextran and a Low-Viscosity Hb-Based O_2 Carrier. *Am. J. Physiol.: Heart Circ. Physiol.* **2004**, *287* (1), H363−H373.
(23) Tsai, A. G.; Cabrales, P.; Winslow, R. M.; Intaglietta, M. Microvascular Oxygen Distribution in Awake Hamster Window Chamber Model during Hyperoxia. *Am. J. Physiol.: Heart Circ. Physiol.* **2003**, *285* (4), H1537−H1545.
(24) Yu, Z.; Xu, Z.; Zeng, R.; Xu, M.; Zheng, H.; Huang, D.; Weng, Z.; Tang, D. D-Band-Center-Engineered Platinum-Based Nanozyme for Personalized Pharmacovigilance. *Angew. Chem., Int. Ed. Engl.* **2025**, *64* (2), No. e202414625.
(25) Yu, Z.; Tang, J.; Gong, H.; Gao, Y.; Zeng, Y.; Tang, D.; Liu, X. Enzyme-Encapsulated Protein Trap Engineered Metal−Organic Framework-Derived Biomineral Probes for Non-Invasive Prostate Cancer Surveillance. *Adv. Funct. Mater.* **2023**, *33* (26), No. 2301457.
(26) Wu, D.; Tang, J.; Yu, Z.; Gao, Y.; Zeng, Y.; Tang, D.; Liu, X. Pt/Zn-TCPP Nanozyme-Based Flexible Immunoassay for Dual-Mode Pressure−Temperature Monitoring of Low-Abundance Proteins. *Anal. Chem.* **2024**, *96* (21), 8740−8746.
(27) Olson, J. S.; Foley, E. W.; Rogge, C.; Tsai, A.-L.; Doyle, M. P.; Lemon, D. D. No Scavenging and the Hypertensive Effect of Hemoglobin-Based Blood Substitutes. *Free Radical Biol. Med.* **2004**, *36* (6), 685−697.
(28) Alayash, A. I. Mechanisms of Toxicity and Modulation of Hemoglobin-Based Oxygen Carriers. *Shock* **2019**, *52* (1S), 41−49.
(29) Segre, G.; Silberberg, A. Behaviour of Macroscopic Rigid Spheres in Poiseuille Flow. Part 2 Experimental Results and Interpretation. *J. Fluid Mech.* **1962**, *14*, 136−157.
(30) Yalcin, O.; Wang, Q.; Johnson, P. C.; Palmer, A. F.; Cabrales, P. Plasma Expander Viscosity Effects on Red Cell-Free Layer Thickness after Moderate Hemodilution. *Biorheology* **2011**, *48*, 277−291.
(31) Elmer, J.; Cabrales, P.; Wang, Q.; Zhang, N.; Palmer, A. F. Synthesis and Biophysical Properties of Polymerized Human Serum Albumin. *Biotechnol. Prog.* **2011**, *27* (1), 290−296.
(32) Belcher, D. A.; Williams, A. T.; Munoz, C. J.; Muller, C. R.; Walser, C.; Palmer, A. F.; Cabrales, P. Attenuating Ischemia-Reperfusion Injury with Polymerized Albumin. *J. Appl. Physiol.* **2022**, *132* (2), 489−496.

https://doi.org/10.1021/acsabm.6c00900
ACS Appl. Bio Mater. XXXX, XXX, XXX−XXX